VTT Technical Research Centre of Finland

Poly(lactic acid)/pulp fiber composites

Paunonen, Sara; Berthold, Fredrik; Immonen, Kirsi

Published in:
Journal of Applied Polymer Science

DOI:
10.1002/app.49617

Published: 10/11/2020

Document Version
Peer reviewed version

Received: 2 March 2020 | Revised: 13 May 2020 | Accepted: 8 June 2020

DOI: 10.1002/app.49617

ARTICLE

Applied Polymer SCIENCE WILEY

Poly(lactic acid)/pulp fiber composites: The effect of fiber surface modification and hydrothermal aging on viscoelastic and strength properties

Sara Paunonen[1] | **Fredrik Berthold**[2] | **Kirsi Immonen**[1]

[1]VTT Technical Research Centre of Finland Ltd, Solutions for Natural Resources and Environment, Tampere, Finland

[2]RISE Research Institutes of Sweden AB, RISE Bioeconomy, Stockholm, Sweden

Correspondence
Sara Paunonen, VTT Technical Research Centre of Finland Ltd, Solutions for Natural Resources and Environment, FI-33101 Tampere, Finland.
Email: sara.paunonen@vtt.fi

Funding information
VTT Technical Research Centre of Finland; RISE Research Institutes of Sweden

Abstract

Poly(lactic acid) (PLA)/kraft pulp fiber (30 wt%) composites were prepared with and without a coupling agent (epoxidized linseed oil, ELO, 1.5 wt%) by injection molding. The non-annealed composite samples, along with lean PLA, were exposed to two hydro-thermal conditions: cyclic 50% RH/90% RH at 23 and 50°C, both up to 42 days. The aging effects were observed by size exclusion chromatography, differential scanning calorimetry, dynamic and tensile mechanical analysis, and fracture surface imaging. ELO temporarily accelerated the material's internal transition from viscous to an increasingly elastic response during the aging at 50°C. ELO also slowed down the tensile strength reduction of the composites at 50°C. These observations were explained with the hydrophobic ELO molecules' coupling and plasticizing effects at fiber/matrix interfaces. No effects were observed at 23°C.

KEYWORDS

aging, biopolymers and renewable polymers, cellulose and other wood products, composites

1 | INTRODUCTION

Aging behavior of materials has a direct impact on their long-term performance, particularly in load-bearing structures, but also in consumer and other products. For new materials such as fully bio-based or biodegradable polymers, it is essential to determine the property space in relation to the polymers commonly used today. For many applications, pure polymers need to be reinforced in order to reach satisfactory mechanical performance. In the case of bio-based polymers, plant fibers are commonly used as reinforcement. This study concentrates on the effects of two environmental loadings; temperature and cyclic relative humidity (RH), on the properties of bio-based and biodegradable PLA/pulp fiber composites over time. Since the focus was on composites, as they would appear in a product, only nonannealed samples were studied.

In general, aging of fiber-reinforced composites occurs via a number of routes due to the multiple components present in the material: matrix, reinforcements, and additives. Composite behavior arises from the inherent properties, interactions and structural arrangement of these components. In this work, the focus was on how the interface between PLA and unbleached and bleached hardwood kraft pulp reinforcement fibers (30%wt) changed as aging progressed, studied through the composite's viscoelastic and tensile properties. The main differences between the pulp types include the degree of lignin and extractives removal, particle size distribution in pulp, and the general pliability of the wood fibers.[1]

Due to their natural origin, composition, and structure, wood pulp fibers react to environmental moisture by shrinking and expanding.[2] The rate of dimensional change is at its highest right after the moisture step change. Therefore, expanding and contracting reinforcement fibers induce internal forces that stress the fiber/matrix interfaces and lead to damages that both mechanically weaken the material and open routes for further moisture penetration (see a comprehensive review[3]). In this study, this hypothesis was tested by two environmental loadings sequences involving cyclic RH. The thermal expansion of wood fibers (~0.03%) at 30°C temperature change is negligible compared with the hygroexpansion (~3%) at 40% RH change.[4] Surface modification of wood fibers with epoxidized linseed oil (ELO) was used to enhance the interfacial adhesion. ELO has the ability to couple cellulosic fibers and the matrix polymer, and thus increase the strength properties of PLA/wood or wood fiber composites.[5–7] This effect arises from ELO's action as a reactive compatibilizer at matrix/fiber interfaces. The reported tensile strength improvements are, for example, 20% for nanocellulose,[7] 9% for microcellulose,[7] and 18% for bleached hardwood kraft pulp reinforcement[6] fibers. These results are for freshly produced, nonaged composites. Epoxidized vegetable oils (EVO) also act as plasticizers by penetrating in between the PLA molecules, thus promoting PLA polymer chain mobility.[8] The results have shown that EVOs are partially[5,9,10] or well[11] miscible with PLA, particularly at low dosages (ca. 5 wt%). Therefore, if EVO is added to the matrix in melt blending, the aim is mainly to improve composite ductility.[5,8,12] Without optimization of fiber and EVO contents, the composite strength is compromised.[13]

PLA shows both temperature-induced (see[14] for overview) and moisture-induced degradation, the latter being the main challenge for large-scale industrial applications at room and outdoor temperatures. Biodegradable aliphatic polyesters, PLA being one, degrade via breakage of the hydrolytically labile ester bonds.[15,16] The acidic byproduct of the breakage auto-catalyzes the degradation process.[17] Water diffuses first into the less-organized amorphous regions, which initiates the degradation. This allows for rearrangement of molecular chains leading to cold crystallization. The proximity of the glass transition temperature (T_g) affects the degradation. At temperatures below T_g, PLA is relatively stable, showing erosion only on the polymer surface,[18] whereas above T_g, the erosion turns into bulk erosion. Additionaly, below T_g, the bulk structure of non-annealed injection-molded PLA is affected by physical aging,[19,20] as the polymer chains immobilized in sudden quenching gradually relax. This manifests as slowly changing material properties, adding to the effects of hydrothermal aging.

In this study, dynamic mechanical analysis (DMA) was used as the tool to probe the micro-mechanical aging effects, with a special focus on the effect of ELO on the reinforcement fiber-matrix interfacial bonding. Direct observation of the interfaces is challenging due to the small size and variation of fibers and interfaces. DMA in varying modes has been employed for studying PLA composites filled with various wood fibers, including wood pulp fibers and their fragments,[21–27] and wood powder/flour ground to different particle sizes.[24,25,28,29] None of these utilized DMA analyses in the context of hydrothermal material aging. In the DMA analysis, the sample is subjected to cyclic deformation in the elastic range. Therefore, the analysis was supplemented by unidirectional tensile testing to provide information on stress–strain behavior at large strains.

In this research, non-annealed samples were exposed to cyclic humidity for 42 days at either 23° or 50°C. The objective was to follow changes in molecular weight (m.w.), glass transition temperature (T_g) and crystallinity of PLA, and mechanical properties of the composites at small and large displacements. The main characterization tests included dynamic scanning calorimetry, size exclusion chromatography, DMA, and tensile testing. The results show that, at 50°C, the pretreatment of reinforcement fibers with ELO affected the m.w. and T_g of the matrix and the mechanical properties of composites compared with nontreated reinforcement fibers.

2 | EXPERIMENTAL

2.1 | Materials

Poly(D,L-lactic acid) (PLA) Ingeo 3052D (NatureWorks, Minnetonka, MN) was the matrix biopolymer. 3052D is a transparent, biodegradable and high-flow grade resin intended for injection molding applications.

Two different pulp fiber types were used as the reinforcement phase, both obtained in never dried form from two Finnish pulp mills. Hardwood (birch) kraft pulp was collected from the pulp production line as unbleached brown pulp (solids content [s.c.] of pulp 13.5%) (code in text and graphs UH) and as final pulp product after all bleaching stages (s.c. 10.8%) (code BH). The unbleached hardwood kraft pulp was collected after the oxygen delignification stage. Table 1 shows fiber dimensions measured by FiberTester (L&W Fiber Tester Plus, Code 912) according to ISO 16065-1:2001. PLA and fibers were collected and used fresh to prepare the composite series. The composite processing steps reduce the average length of UH and BH reinforcement fibers in composites by 33

TABLE 1 Geometrical properties of the raw material fibers

	Fiber length (mm)	Fiber width (μm)	Aspect ratio (–)	Fines content (%)
Unbleached hardwood (UH) Kraft pulp	0.959 ± 0.001	22.75 ± 0.07	42.2	21.4 ± 0.6
Bleached hardwood (BH) Kraft pulp	0.97 ± 0.01	22.800 ± 0.001	42.5	21.5 ± 0.5

Note: Average and *SD*.

and 51%, respectively, and therefore increase the fines content.[6]

Commercial epoxidized linseed oil Vikoflex 7,190 (Arkema, Blooming Prairie, MN) (code in text and graphs ELO or EL) was used as a strength additive. It is used as a plasticizer-stabilizer for industrial polyvinyl chloride (PVC). Typical applications include food packaging and medical products, and construction materials.[30] The EL treatment has been seen to preserve the fiber length of BH reinforcement fibers, but not UH reinforcement fiber.[6]

2.2 | Preparation of composite materials and specimens

To remove the cooking chemical residues, the UH pulp was washed five times by diluting it to 5% s.c. and thickening by draining water to 13% s.c. The coarse fraction (1.3 wt%) was removed and the UH accept was centrifuged to 27% s.c. for additive treatment. The BH pulp was centrifuged to 35% s.c. The fiber cakes were then broken in a Forberg batch mixer (Forberg International, Oslo, Norway). ELO was sprayed at a concentration of 5 wt% of fibers weight onto the fibers while mixing (2 min). The treated fibers were then compacted into granules (4 mm sieve opening size), air dried at 50°C for 30 min, and sealed in plastic bags.

Fiber granules were compounded with PLA at a constant concentration of 30 wt% in a twin-screw extruder (Berstorff ZE 25x48D, KraussMaffei Berstorff, Germany) as 2.7 kg batches. The temperature gradient was 60°C at feeding, rising to 190°C in the subsequent four melting zones. The compounds were air cooled, granulated, and stored in Triplex aluminum bags until use. The composite materials are described in Table 2.

The compounds were injection molded into tensile test specimens (dog bones) with an Engel ES 200/50 HL (Engel, Belgium) machine having a screw diameter of 25 mm and a max volume of 69 cm^3 according to standard ISO 527. The temperatures of the three heating cylinders were 190, 185, and 180°C, and the mold temperature was 33°C. Prior to molding, the composite granules were barrel mixed for 5 min to reduce their surface hairiness (shark skin like surface) via mechanical abrasion. The tensile test specimens were 172 mm long.

TABLE 2 Composition and naming of composite materials

Reinforcement pulp type	Additive	
	None	ELO
None	*PLA(100 wt% PLA)*	–
UH	*UH-REF**	*UH-EL***
BH	*BH-REF**	*BH-EL***

Note: *70 wt% PLA, 30 wt% fiber, **68.5 wt% PLA, 30 wt% fiber, 1.5 wt% ELO.

FIGURE 1 Appearance of aging test specimens (from bottom) REF, UH-REF, UH-EL, BH-REF, BH-EL [Color figure can be viewed at wileyonlinelibrary.com]

The dimensions of the rectangular parallelepiped center section were 4 mm × 10 mm × 80 mm. The specimens were stored in airtight bags shielded from light in ambient room temperature until testing.

2.3 | Aging methodology

In order to speed up the aging, test specimens having average dimensions of 1.9 mm × 4 mm × 120 mm (Figure 1) were laser cut from tensile test specimens with a 75 W Epilog Fusion M2 75W laser-engraving machine (Epilog laser). The speed of cutting, energy level, and frequency were adjusted so that the composites did not burn or melt. The ablation width of the laser beam was approximately 1 mm. Four parallel strips were cut from the middle section, leaving 1 mm edge strips.

The test specimens were aged in a CTS-Temperature test chamber (CTS Gmbh, Hechingen, Germany) (series C23, see Table 3) and Weiss SB11/80/40 (series C50) according to the procedures shown in Table 3. The time lag to reach a new RH set point was 20 min for both the CTS and the Weiss cabinet, followed by a damped

TABLE 3 Aging procedures

Series code	Environmental conditions		Sampling times
	% RH	Temperature	
C23	Cyclic 50% RH/ 90% RH, 24 hr hold time	Constant 23°C	0, 7, 21, 42 days
C50	Cyclic 50% RH/ 90% RH, 24 hr hold time	Constant 50°C	0, 7, 21, 42 days

oscillation period of 45 min for CTS and 17 to 87 min for Weiss. The specimens were placed lying flat on a metal grid shelf.

The hold time in series C23 and C50 was determined based on sorption dynamic pretests of specimens having various thicknesses. Prismatic specimens having a cross-section of 1.9 mm × 3 mm reached a constant weight in 42 hr after a 50/90% RH step change. After 24 hr, over 92% of this weight was gained. From a dried state, the 1.9-mm-thick specimens reached a constant weight in 5 days. After 24 hr, 55% of this constant weight was gained.

All samples were vacuum dried at 50°C for 2 days prior to aging. The specimens were analyzed after a conditioning time of 4 days (12 days for unaged composites) in a standard climate (25°C, 50% RH).

2.4 | Moisture content

Three samples were weighed at the end of 50% RH and subsequent 90% RH cycle for C23 and C50. The measurements were taken 2 weeks after the series completion (at 56 and 63 days, respectively). The samples were vacuum dried at 50°C for 2 days, conditioned in a desiccator, and weighed.

2.5 | Molecular weight

The molecular weight (m.w.) of PLA was determined by size exclusion chromatography (SEC) using tetrahydrofuran (THF) as the mobile phase. The SEC system consisted of a guard column, PLgel 10 μm Guard 50 × 7.5 mm, and three PLgel 10 μm MIXED-B LS 300 × 7.5 mm columns connected in series. The columns were kept at 30°C with a CHM column heater (Waters). The detection was performed using refractive index detector (Waters 410). Calibration was performed using polystyrene standards with molecular weights from 580 to 1,400,000. The calibration points were fitted to a linear function. After dissolving the composite samples in THF and removing the pulp fibers (0.2 μm PTFE syringe filter), the PLA solution was analyzed in a concentration of 5 mg/ml. The data were processed with Cirrus GPC software version 3.1 by Polymer laboratories (Agilent). The detector response was integrated up to 25 min prior to the EL peak.

2.6 | Imaging

Images of fracture surfaces of unaged and fully aged tensile test specimens were recorded with a TM-1000 tabletop scanning electron microscope (SEM) (Hitachi, Tokyo, Japan). Samples were sputter coated with gold plasma without gas for 20 s.

2.7 | Glass transition and crystallinity DSC

Thermograms of unaged and fully aged composites were recorded with a TA AQ20 differential scanning calorimeter (DSC) (TA Instruments, New Castle, DE) under nitrogen atmosphere. A thin, from 3 to 5 mg test piece chip was cut with pliers of each material, and sealed in a standard TZero (TA) aluminum pan and lid. A heat-cool-heat temperature ramping was applied from 0 to 200°C at a constant speed of 10°C/min. Three replicas were tested for unaged samples, and one replica for fully aged samples. Cold crystallization and melting enthalpies and temperatures were extracted from the first heating thermograms.

The crystallinity of PLA in composites (fiber fraction $\Phi = 0.3$) and lean PLA ($\Phi = 1$) was calculated from the melting (ΔH_m), cold crystallization enthalpies (ΔH_{cc}) of the samples from the first heating cycle and melting enthalpy of crystalline PLA ($\Delta H_m^0 = 93.1$ J/g,[6]) by the equation

$$C = \frac{\Delta H_m - \Delta H_{cc}}{\Delta H_m^0 (1 - \Phi)} \quad (1)$$

2.8 | DMA and tensile testing

DMA was conducted with a TA DMA Q800 instruments (TA Instruments, New Castle, DE) in dual cantilever mode (clamp free length 35 mm). Specimens (free L/T ratio 18.4, see Chapter 2.3) were loaded at a frequency of

1 Hz (amplitude 20 μm) while heating from 28 to 130°C. Their approximate cross section dimensions were 1.9 mm × 4.2 mm. Average dimensions were measured with a micrometer prior to testing. One replicate was tested. *SD* was determined by running three replicates for two materials each, and averaging the *SD* for each parameter.

Tensile testing of an aged specimens was run with a universal tensile tester (MTS Systems) in standard climate (25°C, 50% RH). A 2 kN load cell (MTS Systems Norden AB, Eden Prairie, MN) (model 41-0374-03) was used with pneumatic grips (compression force 55 psi). The grip-to-grip distance was 60 mm, and the crosshead speed was 10%/min (6 mm/min). E-modulus values were determined with crosshead displacement. Five replicates were tested.

3 | RESULTS

3.1 | Moisture content

Moisture content (m.c.) gain of PLA-pulp fiber composites, fundamentally arising from their chemical composition, is a result of the temperature-dependent moisture and liquid water diffusion into the constituting components. The experimental setup used in this study, limiting the high humidity level to 90% RH, prevented the samples from exposure to water in liquid state. Figure 2 shows the maximal m.c. changes during the C23 and C50 series. PLA showed affinity for moisture, which is a prerequisite to hydrolysis. At the end of the 50° C aging, the PLA hydrolysis process had reached an advanced state (see Figure 3). Intermediate m.c. measurements would have shown increasing m.c. values for PLA due to the progressing hydrolysis, in particular due to the increase in the number of hydrophilic end groups and thus hydrophilicity of PLA.[17] After a 50% RH step in 50°C, all composites had a m.c. that is relatively low (~1.6 wt%) compared with that after a 90% RH step in 50°C (from 4.26 wt% for BH-EL to 5.07 wt% for UH-REF). The fluctuating moisture level, between 50 and 90% RH, used in the aging procedure, exposed the samples to 42 cycles during which the moisture content varied by roughly 1% at 23°C, and by roughly 3% at 50°C.

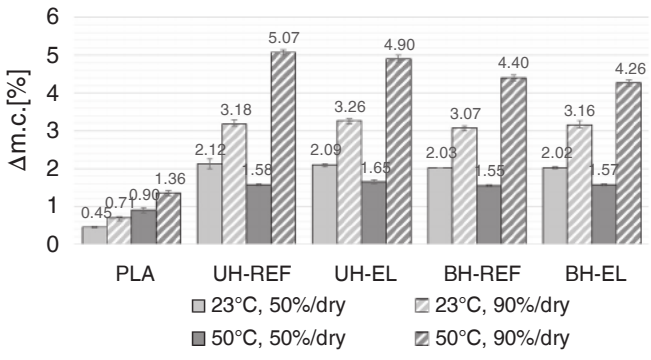

FIGURE 2 Moisture content at cycle end for C23 and C50. Average, and one *SD*

Above a certain fiber content level a percolating fiber network is present in the composite, enabling faster transport of water which directly affects moisture gain.[31] At 30 wt% fiber content, the network connectivity of reinforcement fibers is low,[32] limiting the moisture transport rate mainly to diffusion through PLA and along fiber/matrix interfaces. However, most of the observed moisture uptake in composites was taken up by the fibers, explaining the higher water content of these samples. Bleaching and the EL treatment did not have a major effect on the composite m.c., but at 90% RH, the EL treatment seemed to reduce the m.c. compared with non-treated fibers. Pulp fiber type is not crucial to composite swelling.[27]

3.2 | Molecular weight of PLA

Figure 3 shows the behavior of the weight average molecular weight (M_w) and the molecular weight of the highest peak (M_p) of the PLA reference and the PLA matrices along the two aging treatments. The number average molecular weight (M_n) was sensitive to the chromatogram integration at the low molecular weight end. This caused M_n curves to be nonsmooth for some of the composites. However, M_n showed the same general trends and phenomena as M_w and M_p that are presented in Figure 3. The incorporation of fibers into PLA increases shearing during the injection molding. This resulted in a reduction of molecular weight for all composites at day 0 compared with PLA. In addition, any trace water in fibers would induce hydrolytic degradation that would be seen as a decreasing molecular weight of PLA. Throughout the presented data, the PLA molecular weight of the UH samples was at a lower level than that of the BH samples. The PLA matrices of the UH composites experienced more severe sharing during injection molding due to the 20 bar higher injection pressure that was applied to improve the quality of the tensile test specimens.

During the relatively mild C23 treatment, the M_w and M_p values of PLA declined 7 and 4%, respectively. This is an indication of degradation at high percentage RH, as PLA molecules do not hydrolytically degrade when the sample is stored at 23°C/50% RH.[33] Due to increased shearing, the incorporation of fibers into PLA resulted in a reduction of molecular weight for all composites at day

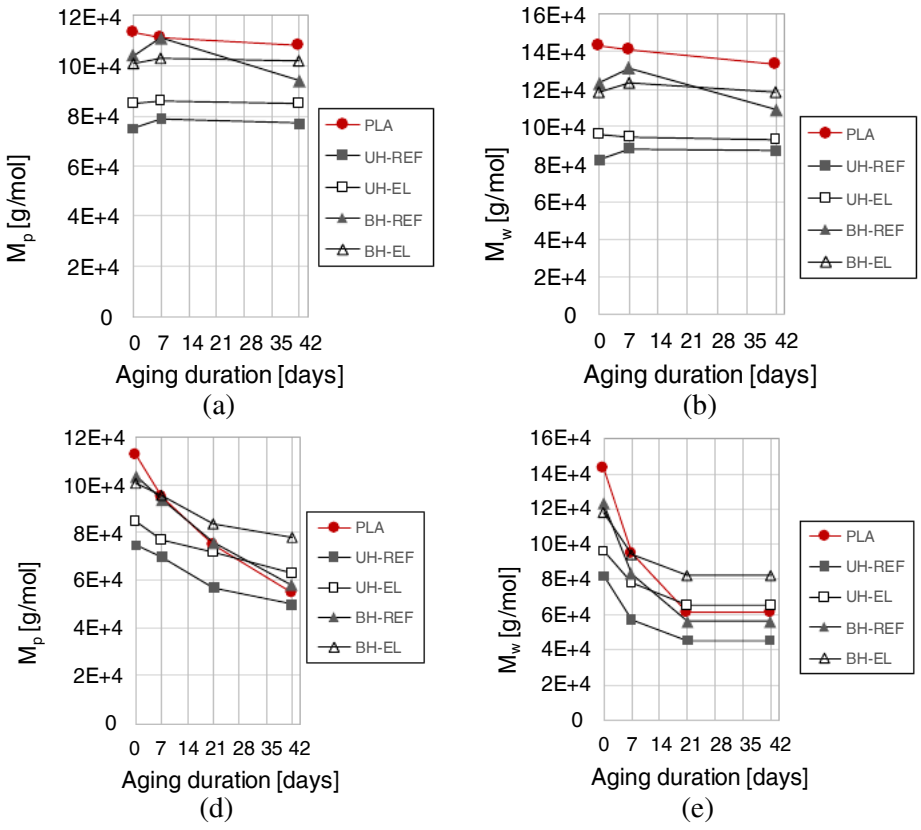

FIGURE 3 M_p and M_w for (a, b) C23, and (d, e) C50, respectively [Color figure can be viewed at wileyonlinelibrary.com]

0. If the reinforcement fibers were unbleached (UH), the EL treatment was able to protect the PLA molecules from breakage in composite manufacturing. This can be seen in M_w and M_p data, and contributes to the higher composite strength properties shown in Figure 9a and Figure 9c compared with bleached BH fibers. During the whole C23 experiment, the M_w and M_p values of all composites were stable, except for BH-REF that seemed to fall. However, in the M_n data (not shown), BH-REF was at the same level as BH-EL and did not show any unexpected behavior.

In the C50 experiment, the PLA degradation was more intensive due to the higher diffusion rate of water, and its solubility to PLA,[17] and the proximity of PLA T_g compared with those in 23° C. The M_w and M_p values of PLA declined 57 and 51%, respectively. The M_w decline reached a plateau, whereas M_p declined in a more linear manner. Initially at day 0, when the PLA crystallinity was low, PLA chains were attacked randomly in the amorphous bulk material. These smaller PLA molecules were then able to orient themselves into crystallites with reduced hydrolysis reactivity. The increasing crystallinity (see Table 4) was able to limit water diffusion and hence, restrict access to hydrolytically labile bonds in the PLA chains in crystallites,[16,17]

Throughout the C50 series, the M_w(PLA) and M_p(PLA) values were higher for the composites with EL-treated reinforcement fibers (UH-EL, BH-EL) than those with non-treated fibers (UH-REF, BH-REF). This advantage persisted throughout the aging, and was even intensified toward the end of it. As an example, for EL-treated and nontreated UH fibers, the difference in M_w(PLA) grew from 17 to 44%, and for EL-treated and non-treated BH fibers, from −4 to 46%. Therefore, ELO protected the PLA molecules in composites from breaking hydrolytically, either via the action of the large molecules it had formed with PLA (and cellulose), or through its hydrophobicity. End capping both ends of PLA chains have several effects that can significantly postpone the hydrolytic degradation.[34] Even at slow dosages, the reaction of ELO with some of the carboxylic end groups of PLA at fiber interfaces may delay water erosion of the PLA polymer by reducing, for example, the autocatalytic effect.[17] Alternatively, the volume that the hydrophobic ELO occupies may slow down the diffusion of water from fibers to PLA, and thus slow down the reduction of observed PLA molecular weight. According to Figure 2, the moisture content reduction by ELO was obvious for 90% RH/50°C cycles.

TABLE 4 T_g (onset), cold crystallization peak temperature (Tcc) and enthalpy (ΔHcc), first and second melting peak temperature (Tm_1st and Tm_2nd), and melting enthalpy (ΔHm) recorded from first heating data shown in Figure 6 at day 42, and crystallinity (Xc) according to Equation (1)

Material/series	*Tg* (°C)	*Tcc* (°C)	*ΔHcc* (J/g)	*Tm_1st* (°C)	*Tm_2nd* (° C)	*ΔHm* (J/g)	*Xc* (%)
REF							
Untr.	55.0 ± 1.0	125.0 ± 1.0	8.8 ± 1.4	–	150.5 ± 0.3	12.1 ± 0.9	3.6 ± 1.0
C23	59.2	123.7	11.1	–	150.6	15.0	4.2
C50	58.6	86.5	6.7	–	152.1	31.7	26.8
UH-REF							
Untr.	53.4 ± 0.9	112.3 ± 1.3	21.9 ± 2.4	146.9 ± 0.3	153.7 ± 0.2	23.3 ± 1.7	2.1 ± 6.4
C23	57.4	105.9	17.4	145.5	153.0	21.2	5.8
C50	58.1	76.5	0.1	–	151.0	21.1	32.2
UH-EL							
Untr.	51.1 ± 0.2	108.0 ± 0.5	18.8 ± 1.8	145.3 ± 0.2	152.5 ± 0.4	21.9 ± 1.5	4.8 ± 4.2
C23	55.2	99.5	17.2	142.6	151.1	18.7	2.2
C50	**	78.3	1.0	–	150.1	19.3	28.1
BH-REF							
Untr.	54.4 ± 0.4	113.7 ± 4.9	17.7 ± 0.9	146.9 ± 0.3	152.8 ± 0.1	20.4 ± 1.0	4.2 ± 2.7
C23	56.2	108.5	18.0	146.2	152.4	18.8	1.2
C50	58.8	86.4	0.6	–	151.2	20.7	30.9
BH-EL							
Untr.	52.3 ± 0.2	107.8 ± 0.5	15.6 ± 1.0	146.0 ± 0.2	152.8 ± 0.2	19.8 ± 1.1	6.5 ± 1.0
C23	54.6	102.3	16.0	144.3	151.4	20.9	7.5
C50	61.4	76.6	0.8	–	150.8	17.9	26.3

Note: Average, *SD* ($N = 3$) for untreated samples (Untr). ** Data not available.

3.3 | Visual examinations of fracture surfaces after tensile testing

Figure 4 shows examples of failure surfaces of PLA, UH-REF, and UH-EL before and after 42 days/C50 treatment. Prior to the aging, the fracture surface on PLA was relatively flat, and occasionally the surface was covered with very thin polymer strains (Figure 4a, arrow), reported also by other researchers,[35] which are a result of plastic deformation. However, after the aging at 50° C, higher sharp ridges tended to form on the fracture surface on PLA (Figure 4d, arrow). Decreasing molecular weight (see Figure 3d for PLA) made the PLA more brittle, which resulted in a sharp, rather than viscous breakage, typically seen as thin strains in fracture surface images (Figure 4a, arrow).

No major visual differences were seen between non-treated and EL-treated UH samples before aging (Figure 4b,c). Fibers perpendicular to the composite fracture surface were not pulled out in either of the samples, which indicates a good surface adhesion. The length and appearance of exposed fiber sections shown in Figure 4e,f indicate that after the C50 treatment a bigger force was needed to break the EL-treated UH sample compared with the nontreated one. This was also seen in tensile test results shown in Figure 9c Figure 4e shows how very long exposed fiber segments are protruding from the UH-REF fracture surfaces close to the sample edge, proving for a radical loss of interfacial strength. The general appearance of aged UH-EL (see Figure 4f) is the same as before the aging. The one exposed fiber segment (see Figure 4f, arrow) is damaged, also indicating that a big force was needed to pull it out from the matrix.

Figure 5 shows representative images of UH-REF and UH-EL fracture surfaces at larger magnification. No major gaps were detected at the fiber-matrix interface for either of the samples. However, without EL treatment, fibers could be pulled out before the fracture. The EL treatment thus preserved the integrity of the composite interface during aging.

The prismatic test specimens were laser cut from standard-size tensile test specimens. Due to this

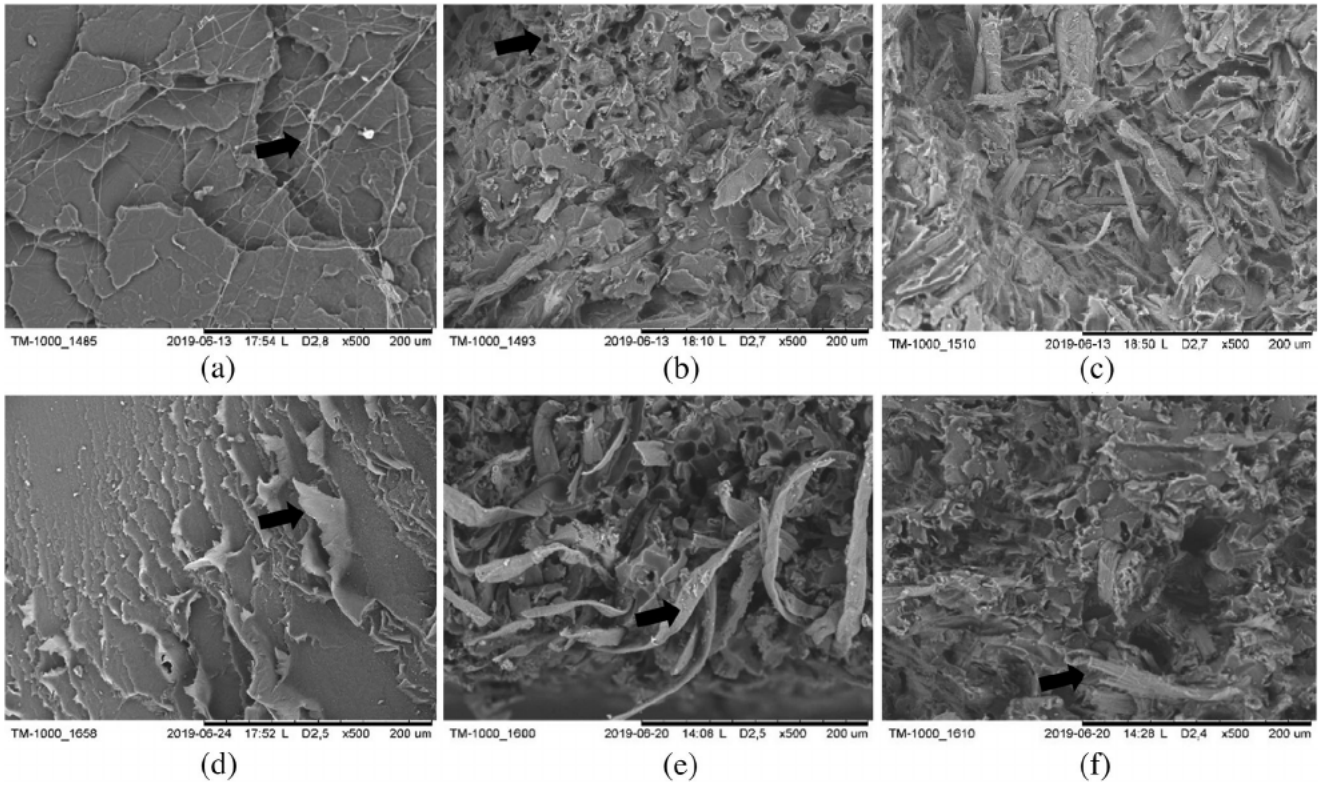

FIGURE 4 SEM images (×500) of fracture surfaces before (a–c),and after (d–f) the C50 treatment for samples: (a,d) PLA, (b,e) UH-REF, and (c,f) UH-EL. Figures (b,e) taken close to specimen edge. Arrows in figures: (a) thin polymer strains, (b) porous layer near specimen edge, (d) sharp PLA ridges, (e) exposed, undamaged fiber segment, (f) exposed, slightly damaged fiber segment

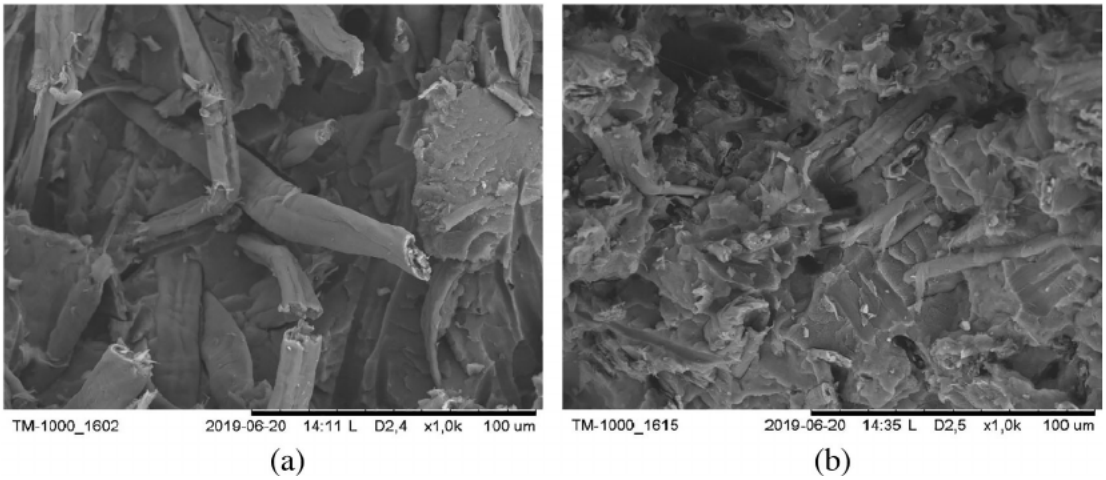

FIGURE 5 SEM images (×1,000) of (a) UH-REF, and (b) UH-EL after the C50 treatment, highlighting how EL affects the fiber pull-out

treatment, the largest faces of all the composite specimens had a porous surface down to the depth of ~0.2 mm (see Figure 4b for an example, arrow). The heat of laser cutting evaporated any traces of moisture from the surface fibers, leading to holes in the matrix. The pores provided a pathway for moisture to penetrate into the composite specimens during aging. Such a porous layer was not seen in PLA specimens.

3.4 | Glass transition temperature and crystallinity via DSC

Figure 6 shows the first heating thermograms for the unaged and fully aged PLA and composite specimens. By visual inspection, aging affected T_g, cold crystallization temperature and enthalpy and crystallite melting behavior. Table 4 summarizes the thermal properties in tabular form.

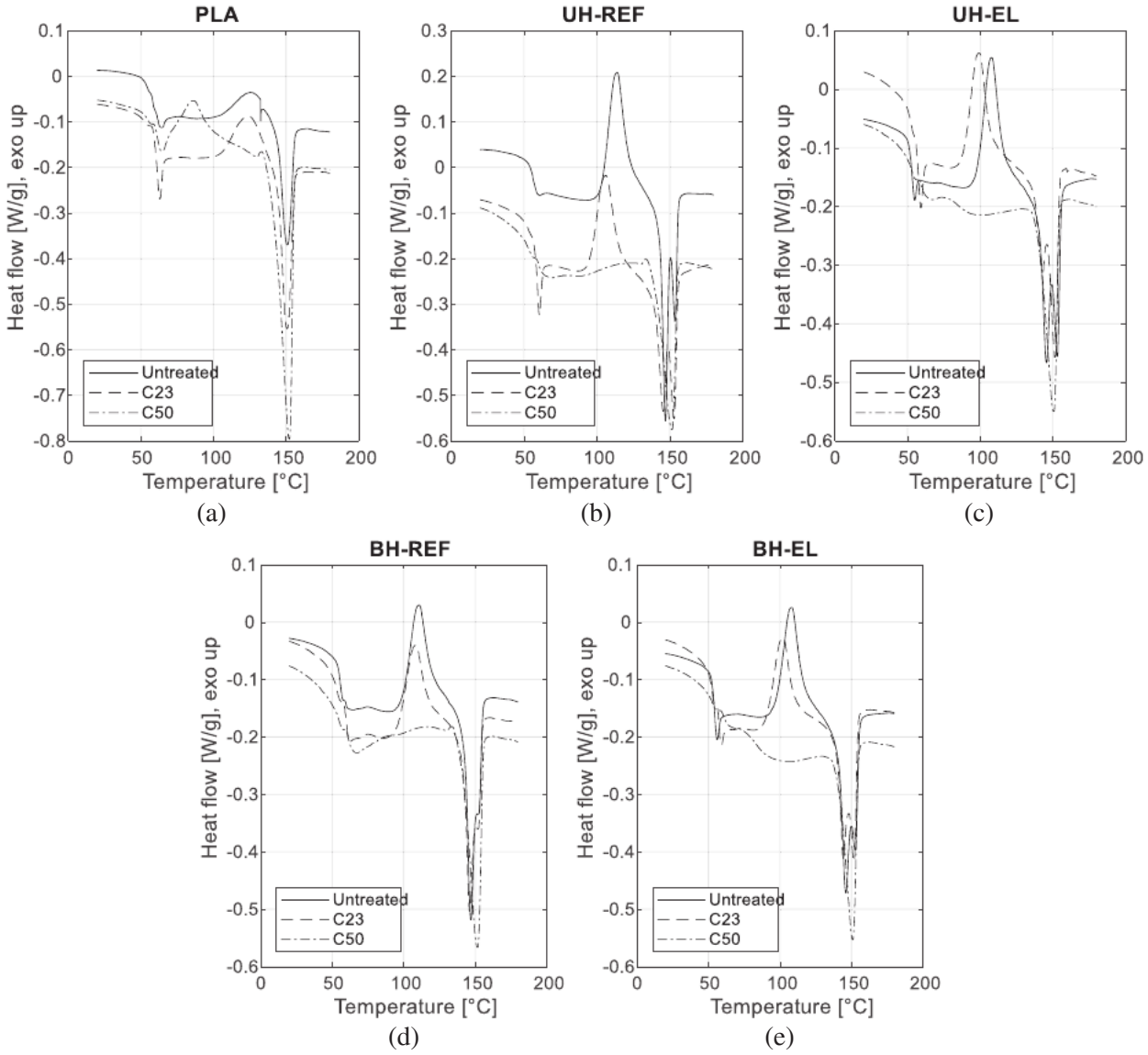

FIGURE 6 DSC thermograms from first round heating at 10°C/min for (a) PLA, (b) UH-REF, (c) UH-EL, (d), BH-REF, and (e) BH-EL. Due to the composite manufacturing process, the composite samples showed dual-peak melting behavior

Usually reinforcement fibers show limited increasing or decreasing effect on the T_g of the polymer matrix. The UH and BH fibers slightly reduced the T_g of nonaged PLA, as was also noted for the same composite types by Peltola et al.[6] The introduction of EL further reduced the T_g of (nonaged) composites, potentially due to the plasticizer functionality of the ELO molecules. In contrast, the C23 and C50 increased the T_g of all samples. As Figure 2 shows, both C23 and C50 involved an induction of moisture in the material, leading to PLA degradation. The increasing T_g is due to the constraining effect of the increasing crystallinity. In the C23 experiments, the T_g(PLA) was increased by 4.2°C and the T_g(UH-REF) and T_g(UH-EL) both by 4°C and the T_g(BH-REF) and T_g(BH-EL) by ~2°C. The C50 increased the T_g(BH-EL) by as much as 9.1°C compared with untreated BH-EL.

Hydrolytic aging in 50°C (C50) shifted the PLA cold crystallization (CC) process to lower temperatures (peak Tcc from 125.0 to 86.5°C), as also observed by others.[36] The oligomeric lactic acid chains that were formed in the hydrolytic PLA chain scission are more likely to move and thus crystallize at lower temperatures.[36] Traces of this PLA CC peak were seen for the C50-aged composites, especially in the presence of ELO (see Table 4 and Figure 6c,e), proving the presence of these crystallites also in the composite samples. However, the lack of distinct CC in composites aged at 50°C suggest comprehensive crystallization caused by decreased molecular weight.

The original calculated crystallinity of lean, injection-molded amorphous 3052D was low (3.6 ± 1.0), but still slightly higher than in previous work experimenting with the same composite types.[6] The C23 treatment did not

affect the crystallinity (see Table 4). However, after the C50 treatment, lean PLA had a degree of crystallinity of approximately 27%, and the PLA matrices from 26 to 32%. The data in Table 4 suggests that ELO decreased the level of crystallinity by 4% points in samples aged in 50°C. This can be explained by the hindering effect that the EL molecules posed to the rearrangement of PLA molecules. The crystallinity degree of PLA and the crystallite morphology contribute to the mechanical properties of matrix material in composites, increasing crystallinity contributing to better mechanical properties. However, due to the multitude of other factors affecting composite mechanical properties during aging, such as molecular weight of PLA, no straightforward effects of PLA crystallinity can be observed on the mechanical properties shown in Figure 9.

Another interesting phenomenon was related to the crystalline PLA fraction and its melting in heating. In the first heating, all untreated and C23-treated composites showed a dual-peak melting behavior, which they all lost after the C50 treatment (see Table 4 for Tm_1st and Tm_2nd and Figure 6). Pure PLA had a single first melting peak before and after C23 and C50 treatments approximately at the same temperature. The dual melting peak in composites potentially arises due to polymer chains losing their alignment during melt mixing of PLA and fibers, or due to the presence of two crystallite populations with varying thermal stability.[37] The crystallites created in the composite manufacturing had a melting point from 7 to 9°C lower than that of crystallites in lean PLA. Based on observed melting temperatures, it is particularly crystallites melting at a lower temperature that the C50 aging removes, suggesting that they have rearranged into a more stable form during aging. After aging at 50°C, neither PLA(neat) nor PLA(composite) exhibit Tm_1st.

3.5 | Dynamic mechanical properties (DMA)

Polymer chain mobility in bulk and polymer-fiber interactions were studied by measuring storage modulus (E′), loss modulus (E″) and the loss factor (tan δ) in a temperature sweep at 1 Hz as a function of aging.

The glass transition (T_g) is a relaxation phenomenon that can be determined from all three curves (E′, E″, tan δ) produced by a DMA apparatus.[38] Figure 7 shows the temperature (T) at peak tan δ, which gives the highest T_g estimate of these three methods. The advantage regarding tan δ (ratio E''/E') is that it is independent of geometry effects.[38] Therefore, the determinations are accurate even for uneven test specimen, and reliable comparisons among a specimen set are possible. Figure 7 shows the combined effect of hydrothermal and physical aging on T_g. Throughout the C23 aging (Figure 7a), the T_g remained relatively stable for both PLA and the composites, indicating that no major molecular events that would have affected the viscoelastic behavior were occurring at 23°C. However, the curves confirm the results shown in Table 4 that the ELO treatment reduced the T_g compared with nontreated composites.

In contrast, during the C50 aging treatment, the composites with and without the ELO treatment show different dynamics of T_g development, see Figure 7b. In general, as the crystallinity of PLA increased along the progressing hydrothermal aging, also the T_g of PLA increased.[39] The rate of T_g change is dependent on the temperature and also the presence or absence of ELO treatment. The UH-EL and BH-EL curves even suggests that the T_g might even reach a plateau. This same overall behavior was detected also in T at E′ onset, and T at peak E″ data, the two other T_g values obtained from the DMA data (not shown).

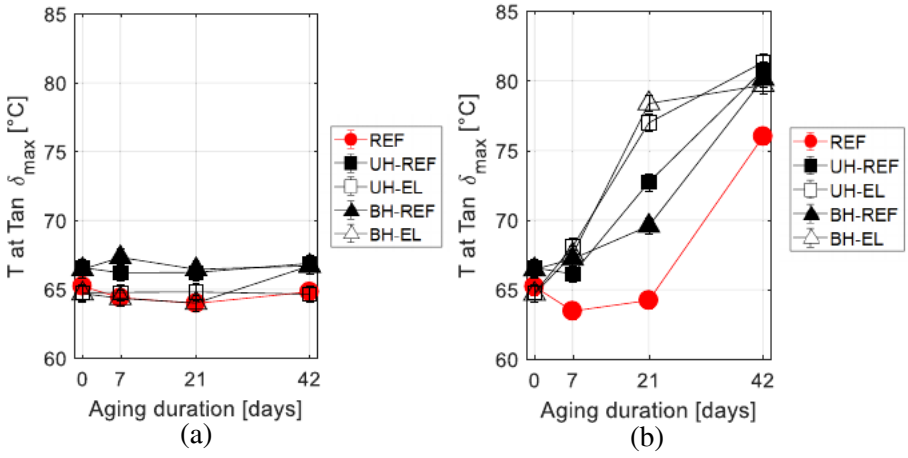

FIGURE 7 T at peak tan δ for (a) C23, and (b) C50 [Color figure can be viewed at wileyonlinelibrary.com]

In search of further evidence on the effects of ELO, the peak tan δ values were plotted as a function of aging (Figure 8). This damping factor shows the ratio of energy dissipation through, for example, segmental motions of polymer chains and material's internal friction, and the recoverable elastic energy. The peak value is the turning point from glassy to rubbery behavior. The fibers and fiber fragments posed a hindrance to the PLA molecular movement in composites, which can be seen as lower overall level of peak tan δ values for composites in Figure 8. At 23°C, the peak tan δ for composites is unchanged, being in accordance with other results, such as the relatively unchanging tensile strength show in Figure 9a. The initial 15% drop in peak tan δ for pure PLA at 23°C could be attributed to physical aging. After this initial drop, the internal molecular structure of PLA did not change significantly, and the peak tan δ remained more or less unchanged.

In the C50 experiment (Figure 8b), the molecular weight was decreasing (Figure 3d,e), which increased the polymer chain mobility, leading to faster crystallization. As the crystallinity content increased considerably, PLA started to act more elastically due to the constraints the crystal regions exerted on the amorphous region mobility. Therefore, the recorded peak tan δ value was reduced and T at peak tan δ (Figure 7b) increased. Adding reinforcement fibers considerably reduced the peak tan δ of PLA, as PLA chains were interacting with fiber surfaces. From day 0, the peak tan δ of also PLA matrices started to decline, but at a smaller rate than that of PLA. The fibers therefore slowed down the shift to elastic behavior. Throughout the aging, UH-REF showed slightly more elasticity compared with BH-REF (see Figure 8b), potentially due to stronger interactions and interfaces between the lignin-rich fiber surface and PLA, or due to unbleached fibers encouraging crystallization of PLA.[6] Table 4 shows how UH-REF (32.2%) had a little higher crystallinity than BH-REF (30.9%). The fact that epoxidized linseed oil reduced the peak tan δ even further, is an indication of its ability to reinforce the interfaces, as can be seen in Figure 5. The reinforcement advantage lasted for ∼21 days in cyclic humidity at 50°C, and was lost at 42 days. This may be due to the evolving hydrolytic degradation and shortening of the PLA chains at interfaces and in PLA bulk. Even if the PLA-ELO-cellulose couplings were resistant to the hydrolytic environment at 50°C, the interfaces may have lost their strength due to ever-shortening PLA chains. At T at peak tan δ, E′ of PLA had dropped over 90% and E′ of the composites over 80% compared with their E′ at 23°C.

3.6 | Tensile mechanical properties

Figure 9 shows the ultimate tensile strength and E-modulus as a function of aging. As expected, reinforcement fibers increase the values of both parameters throughout the experiments compared with lean PLA. However, the reduction of the E-modulus during the aging is a contribution of the fibers, as the E-modulus of lean PLA remains stable (see Figure 9b,d). For both experiments C23 and C50, the overall reduction of the E-modulus of composites is ∼15%, and the reduction is independent of the temperature. The EL treatment did not affect the rate of E-modulus decline.

The tensile strength of PLA was relatively unchanged during C23, indicating the high stability of the composites under those conditions, as was also shown by the DMA results (see Figures 7 and 8a). During C50, however, the tensile strength of PLA was severely impaired at 21 days, reaching a reduction of 50% in 42 days. The repeated m.c. changes of PLA during this time were only 0.5% (see Figure 2), but it induced severe reduction of molecular weight (Figure 3c,d) and thus strength loss.

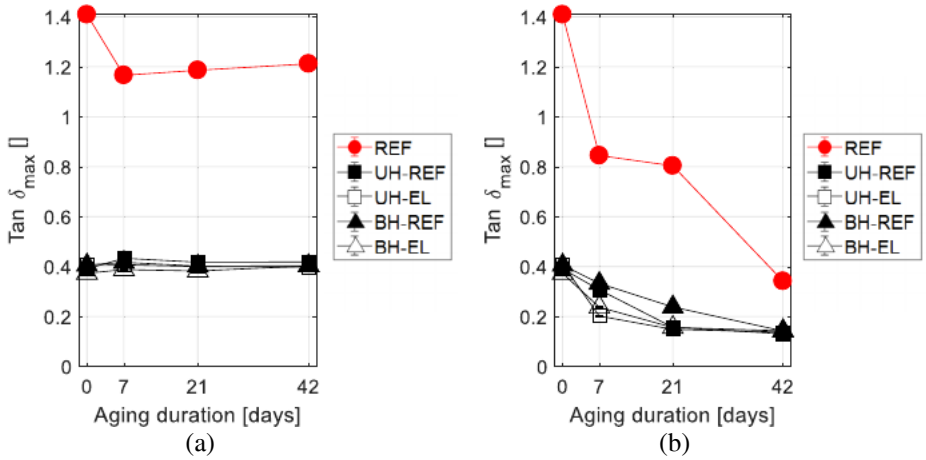

FIGURE 8 Peak tan δ C for (a) C23, (b) C50 [Color figure can be viewed at wileyonlinelibrary.com]

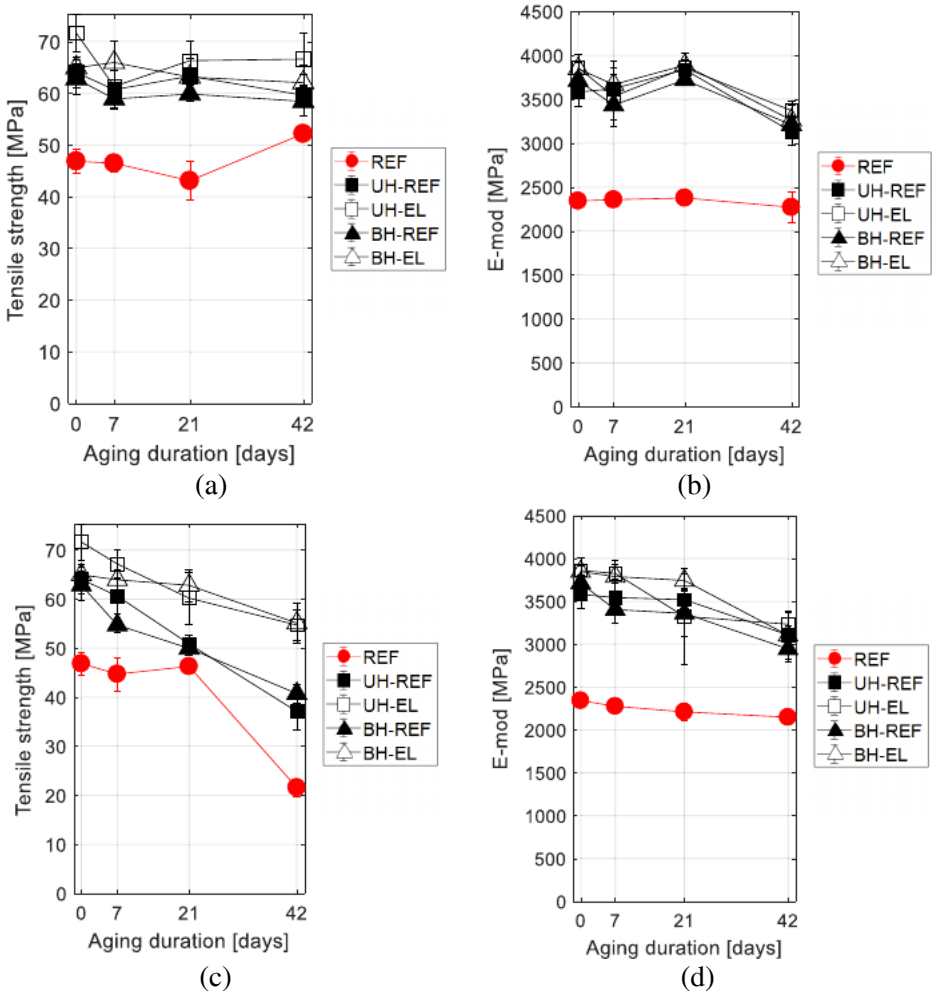

FIGURE 9 Tensile strength, and E-modulus for (a, b) C23 series, and (c, d) C50. Average and *SD* ($N = 5$) [Color figure can be viewed at wileyonlinelibrary.com]

The fiber reinforcement and EL treatment counteracted the decline with varying rates (Figure 9c). The low dosage of ELO on fiber surfaces (5 wt% of fibers) slowed down the tensile strength loss of composites. For unbleached fibers, the strength loss percentage over 42 days was reduced from 42 to 24% due to EL, and for bleached fibers from 35 to 15%, compared with 54% for PLA. It has been shown that epoxide-based surface treatments slow down the degradation of mechanical properties; the results presented for storage modulus, of PLA/cellulose powder composites during aging in constant humidity conditions.[35]

Several mechanisms explain ELO's ability to slow down the strength reduction. The epoxide groups in ELO molecules are able to bridge cellulose and PLA molecules by forming covalent bonds with hydroxyl groups in PLA and cellulose,[8] and thus strengthen the fiber-matrix interfaces. Thus, ELO acts as a bridge connecting PLA and cellulose creating stronger interfaces along the specimen length, which manifests as a higher tensile strength. Carboxylic end groups in PLA have the ability to auto catalyze the hydrolytic degradation process.[15] When ELO reacts with hydroxyls in PLA carboxyl groups,[8] this protects the PLA chains and reduces their degradation rate. Additionally, the plasticizing effect of EL is based on its ability to occupy free volume within and between PLA molecules.[8] As the space is occupied with hydrophobic ELO molecules, less water molecules will penetrate the PLA matrix from fibers through the interfaces, which in turn decreases the degradation of PLA in the interfaces and in the bulk. Epoxidized vegetable oil has been shown to increase hydrophobicity of cellulose fibers, due to epoxy groups anchoring the hydrophobic triglycerides of ELO into hydrophilic cellulose.[40] At high temperatures (above 100°C), covalent bonding is achieved without catalyst.[7,40] Together, the formation of covalent bonds at the interfaces and the decreased free volume available for water help explain how EL-treated samples maintained strength after aging at 50°C. Further evidences of this shielding effect of PLA-ELO molecules against PLA degradation were seen in PLA m.w. (Ch 3.3.) and m.c. (Ch 3.1) results. E-modulus is a manifestation of slight tightening of the molecular structure of the material during straining, including fibers, interfaces, and the matrix.

ELO did not show any clear shielding effect in the E-modulus data. In 23°C, all the measured parameters were relatively stable, and changes between EL-treated and non-treated samples cannot thus be expected. The data from the C50 experiment (Figure 9d) suggest that the transient interface reinforcement effect of EL treatment seen in the dynamic mechanical parameters (Figures 7b and 8b) could also be seen in the E-modulus. Unfortunately, the deviation in the dataset was high.

In the original hypothesis, the focus was strongly on reinforcement fibers and the mechanical straining effects that their hygroexpansion and shrinking fibers would impose on the fiber/matrix interfaces. The fluctuating m. c. of fibers was straining the interfaces, but the collected data did not allow for conclusions to be made on the effects this had on the composites during aging at 23 and 50°C. Rather, as the fiber network connectivity was low, the presence of the coupling agent/plasticizer ELO on the interfaces affected the moisture diffusion through them, and therefore the hydrolytic degradation of PLA. This manifested as changes in viscoelastic and mechanical properties of the composites.

4 | SUMMARY

In this work, the effect of pulp fiber surface treatment with epoxidized linseed oil on properties of PLA/pulp fiber composites was studied as a function of hydrothermal aging. The two aging treatments involved exposure to cyclic relatively humidity (50/90% RH) in either 23 or 50°C for 42 days.

The results show that ELO influenced the development of viscoelastic properties of composites during the aging in 50°C. As an example for composites with ELO-treated bleached fibers, the temperature of damping peak was 11% higher at 21 days, and the damping peak 27% smaller at 7 days compared with nontreated fibers. At 42 days, no differences were observed in these properties between ELO-treated or nontreated reinforcement fiber composites. This indicates that composites changed their overall structural and damping behavior faster when ELO was present than when it was absent. Furthermore, the ELO treatment slowed down the tensile strength loss of composites during the 50°C aging phase. The strength loss percentage in 42 days was reduced due to ELO by 18 percentage points for unbleached fibers, and by 20% points for bleached fibers. The aging in 23°C did not affect the measured viscoelastic or mechanical properties.

The reduced strength loss reduction and changes in viscoelastic behavior can be explained via the effects of the ELO treatment on fiber surfaces. ELO both strengthens fiber/matrix interfaces via molecular bonds, and occupies free volume within PLA molecules. Due to this, water cannot penetrate the interface volumes, which shields the PLA molecules participating in interfaces and the surrounding PLA molecules against hydrolytic degradation. This conclusion was supported with molecular weight measurements. For ELO-treated UH and BH fibers, the M_p of PLA matrix was reduced by 26 and 23%, respectively, whereas for non-treated UH and BH fibers, the M_p reduction was 33% and 44%, respectively, after 42 days at 50° C. For PLA, the M_p reduction was 51%. The strengthening effect of EL treatment on fiber/matrix interfaces was clearly seen in visual images of exposed fiber segments at the end of aging in 50°C. In addition, ELO's reaction with PLA carboxylic groups caps PLA chain ends and thus reduces the erosion of PLA locally at the interfaces. The bleaching of fibers had an effect on molecular weight, glass transition and other thermal properties of PLA matrix in 50°C aging, but not on the measured mechanical and viscoelastic properties of the composites.

5 | PRACTICAL IMPLICATIONS

The susceptibility of polylactide to degrade under hydrolytic conditions has been of interest for biomedical and packaging applications for a long time. Therefore, the degradation of PLA under physiological and composting conditions has been much studied. Much less effort has been put to study the long-term performance under conditions that resemble usage of products in, for example, construction and transport. As aging studies under real conditions can take several years, procedures to accelerate aging under these conditions are often performed to estimate the service life of products.

This work increased our understanding on how fully biobased composites age under accelerated conditions that simulate moderate and severe climate conditions. Similar studies to show the aging behavior of PLA/hardwood kraft pulp composites have not been published before. Treating the fibers with epoxidized linseed oil considerably slowed down the composite strength degradation, and made the changes in viscoelastic behavior faster. In humid conditions, reinforcement fibers had some added benefit of being able to compensate the PLA degradation even without further hydrolytic stabilization.

ACKNOWLEDGMENTS

The authors would like to thank Mr. Upi Anttila (VTT) and Mr. Eino Sivonen (VTT) for the preparation of the composite samples, and a number people at RISE Bioeconomy; Dr. Kristoffer Segerholm, Dr. Prashanth Srinivasa, Mr. Henrik Pettersson, Mr. Jens Haraldsson,

Ms. Anna Östberg, Ms. Erika Back, for their help executing the experimental work in Stockholm in the spring 2019. The authors gratefully acknowledge the funding from VTT and RISE.

CONFLICT OF INTEREST

The authors declare no conflict of interest.

ORCID

Sara Paunonen https://orcid.org/0000-0003-0554-1570

REFERENCES

[1] P. Bajpai, *Environmentally Friendly Production of Pulp and Paper*, Wiley, Hoboken, New Jersey **2010**.
[2] A. Célino, S. Fréour, F. Jacquemin, P. Casari, *Front. Chem.* **2014**, *43*, 1.
[3] T. H. Mokhothu, M. J. John, *Carbohydr. Polym.* **2015**, *131*, 337.
[4] T. Uesaka, *Handbook of Physical Testing of Paper*, Vol. 1, Marcel Dekker, Inc., New York, Basel **2002** pp 115.
[5] B. W. Chieng, N. A. Ibrahim, Y. Y. Then, Y. Y. Loo, *Molecules* **2014**, *19*, 16024.
[6] H. Peltola, K. Immonen, L. S. Johansson, J. Virkajärvi, D. Sandquist, *J. Appl. Polym. Sci.* **2019**, *136*, 47955.
[7] K. Immonen, P. Lahtinen, J. Pere, *Bioengineering* **2017**, *4*, 13.
[8] J. F. Balart, V. Fombuena, O. Fenollar, T. Boronat, L. Sánchez-Nacher, *Compos. Part B Eng.* **2016**, *86*, 168.
[9] F. Ali, Y.-W. Chang, S. C. Kang, J. Y. Yoon, *Polym. Bull.* **2009**, *62*, 91.
[10] V. S. Giita Silverajah, N. A. Ibrahim, N. Zainuddin, W. M. Z. Wan Yunus, H. A. Hassan, *Molecules* **2012**, *17*, 11729.
[11] E. A. J. Al-Mulla, W. M. Z. W. Yunus, N. A. B. Ibrahim, M. Z. A. Rahman, *J. Mater. Sci.* **2010**, *45*, 1942.
[12] Y. Q. Xu, J. P. Qu, *J. Appl. Polym. Sci.* **2009**, *112*, 3185.
[13] X. Meng, V. Bocharova, H. Tekinalp, S. Cheng, A. Kisliuk, A. P. Sokolov, V. Kunc, W. H. Peter, S. Ozcan, *Mater. Des.* **2018**, *139*, 188.
[14] K. Jamshidi, S. H. Hyon, Y. Ikada, *Polymer (Guildf)*, **1988**, *29*, 2229.
[15] M. A. Elsawy, K. H. Kim, J. W. Park, A. Deep, *Renew. Sustain. Energy Rev.* **2017**, *79*, 1346.
[16] L. N. Woodard, M. A. Grunlan, *ACS Macro Lett.* **2018**, *7*, 976.
[17] G. L. Siparsky, K. J. Voorhees, F. Miao, *J. Environ. Polym. Degrad.* **1998**, *6*, 31.
[18] Y. Aso, S. Yoshioka, A. Li Wan Po, T. Terao, *J. Control. Release* **1994**, *31*, 33.
[19] J. M. Hutchinson, *Prog. Polym. Sci.* **1995**, *20*, 703.
[20] P. Pan, B. Zhu, Y. Inoue, *Macromolecules* **2007**, *40*, 9664.
[21] H. Ren, Y. Zhang, H. Zhai, J. Chen, *Cellul. Chem. Technol.* **2015**, *49*, 641.
[22] F. X. Espinach, S. Boufi, M. Delgado-Aguilar, F. Julián, P. Mutjé, J. A. Méndez, *Compos. Part B Eng.* **2018**, *134*, 169.
[23] Q. Zhang, L. Shi, J. Nie, H. Wang, D. Yang, *J. Appl. Polym. Sci.* **2012**, *125*, E526.
[24] A. P. Mathew, K. Oksman, M. Sain, *J. Appl. Polym. Sci.* **2005**, *97*, 2014.
[25] D. Battegazzore, J. Alongi, A. Frache, *J. Polym. Environ.* **2014**, *22*, 88.
[26] D. Åkesson, T. Vrignaud, C. Tissot, M. Skrifvars, *J. Polym. Environ.* **2016**, *24*, 185.
[27] K. M. Almgren, E. K. C. Gamstedt, *Interfaces* **2010**, *17*, 845.
[28] Y. Altun, M. Dogan, E. Bayraml , *J. Polym. Environ.* **2013**, *21*, 850.
[29] M. Hrabalova, A. Gregorova, R. Wimmer, V. Sedlarik, M. Machovsky, N. Mundigler, *J. Appl. Polym. Sci.* **2010**, *118*, 1534.
[30] Arkema Vikoflex(R) 7190 product sheet. https://tinyurl.com/yy9844gr.
[31] J. George, S. S. Bhagawan, S. Thomas, *Compos. Sci. Technol.* **1998**, *58*, 1471.
[32] W. Wang, M. Sain, P. A. Cooper, *Compos. Sci. Technol.* **2006**, *66*, 379.
[33] J. R. Rocca-Smith, N. Chau, D. Champion, C. H. Brachais, E. Marcuzzo, A. Sensidoni, F. Piasente, T. Karbowiak, F. Debeaufort, *Food Chem.* **2017**, *236*, 109.
[34] D. M. Bigg, *Adv. Polym. Technol.* **2005**, *24*, 69.
[35] H. Kyutoku, N. Maeda, H. Sakamoto, H. Nishimura, K. Yamada, *Carbohydr. Polym.* **2019**, *203*, 95.
[36] J. F. Balart, N. Montanes, V. Fombuena, T. Boronat, L. Sánchez-Nacher, *J. Polym. Environ.* **2018**, *26*, 701.
[37] A. P. Johari, S. Mohanty, S. K. Kurmvanshi, S. K. Nayak, *ACS Sustain. Chem. Eng.* **2016**, *4*, 1619.
[38] K. P. Menard, *Dynamic Mechanical Analysis: A Practical Introduction*, CRC Press, Taylor & Francis Group, Boca Raton, FL, US **2008**.
[39] N. Jiang, T. Yu, Y. Li, *J. Polym. Environ.* **2018**, *26*, 3176.
[40] X. Huang, A. Wang, X. Xu, H. Liu, S. Shang, *ACS Sustain. Chem. Eng.* **2017**, *5*, 1619.

How to cite this article: Paunonen S, Berthold F, Immonen K. Poly(lactic acid)/pulp fiber composites: The effect of fiber surface modification and hydrothermal aging on viscoelastic and strength properties. *J Appl Polym Sci*. 2020;e49617. https://doi.org/10.1002/app.49617